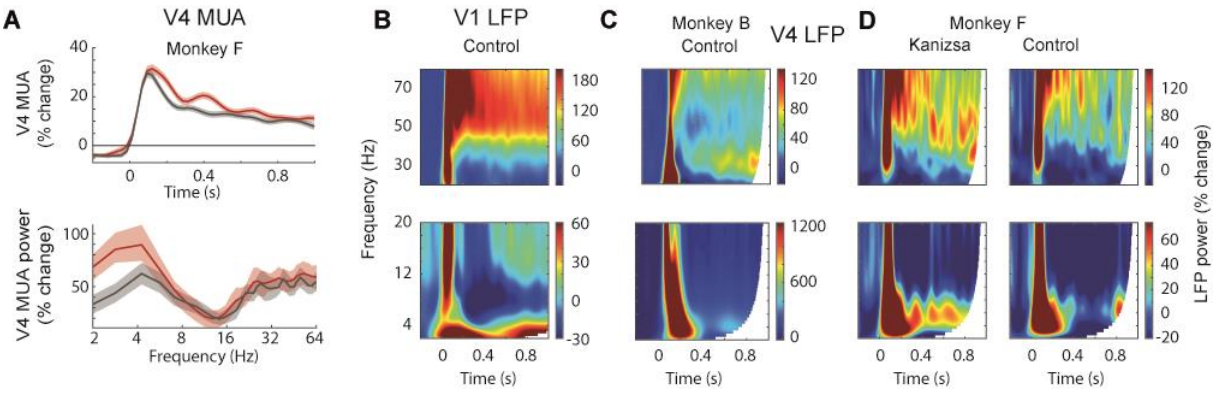

Figure S1. Theta and gamma oscillations in V1 and V4. Related to Figure 1.

(A) Same as Figure 1C, but for monkey F. Upper panel: example V4 MUA response from one representative electrode channel; lower panel: MUA powerspectrum for area V4 averaged across channels from monkey F. Kanizsa (red) and control conditions (gray), shaded areas depict SEM.

(B) Same as Figure 1D, but for the control condition. Time-frequency representations of V1 LFP, averaged across channels from monkey K for the control condition for low (lower panel) and high frequencies (top panel).

(C) Same as Figure 1E, but for the control condition. Time-frequency representations of V4 LFP, averaged across channels from monkey B for the control condition for low (lower panel) and high frequencies (top panel).

(D) Time-frequency representations of V4 LFP, averaged across channels from monkey F for the Kanizsa (left panels) and control condition (right panels) for low (lower panel) and high frequencies (top panel).

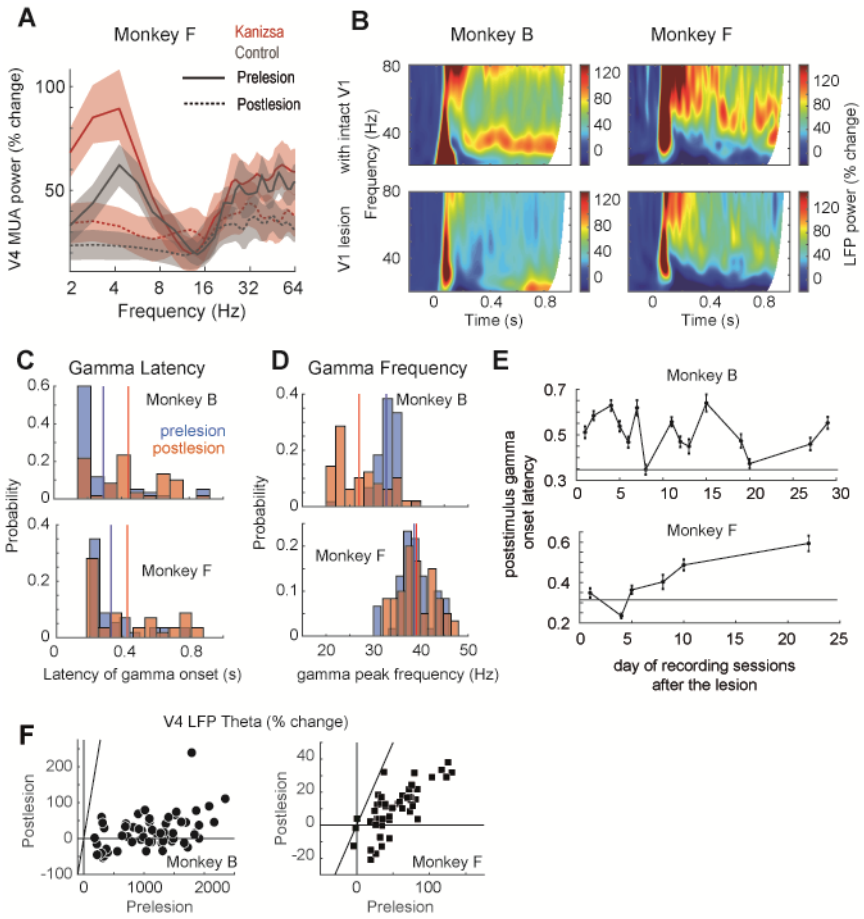

Figure S2. V4 theta and gamma oscillations after V1 lesion. Related to Figure 4.

(A) Same as Figure 4B, but for monkey F. MUA powerspectrum averaged across channels from monkey F for Kanizsa illusion (red) and control condition (gray) pre- (solid lines) and postlesion (dashed lines), showing the elimination of theta activity. Shaded areas depict SEM

(B) Time-frequency representations of V4 LFP, averaged across channels from monkey B (left panels) and monkey F (right panels) before (upper panels) and after the V1 lesion (lower panels). Note the presevation and delayed onset of gamma ocillations after the lesion.

(C) Histograms showing the distribution of the gamma onset latencies after stimulus onset across LFP channels for monkey B (upper panel) and monkey F (lower panel) before (blue) and after the lesion (orange). Vertical lines highlight mean values.

(D) Same as **(C)** but for gamma peak frequencies.

(E) Poststimulus gamma onset latencies as a function of postlesional recording sessions (e.g. day 1 = first recording session of the described experiments after the V1 lesion, not the first day after the lesion) averaged across LFP channels for monkey B (upper panel) and monkey F (lower panel). Horizontal lines depict prelesional mean latencies. Errorbars depict SEM.

(F) Same as Figure 4 G, left panel, but presenting data from both monkeys separately as scatter plots depicting V4 LFP theta power change distributions pre vs. postlesion for monkey B (left panel) and F (right panel). Each dot/square represents data from a single channel, averaged across trials.

Table S1. MUA statistics with intact V1. Related to Figure 1.

Area	MUA increase for Kanizsa condition (mean ± SEM)	MUA increase for control condition (mean ± SEM)	Statistics (illusion > control, Wilcoxon paired signed rank test)	Related Figures
V1 (monkey K)	10.1±1.29%	9.4±1.36%	p=0.07, n=61	Figure 1B
V4 (monkey B)	18.1±1.15%	14.9±1.17%	p=6.6x10^{-6}, n=59	Figure 1C (upper panel), Figure 4E-F, left panels and wings)
V4 (monkey F)	7.7±0.76%	6.9±0.77%	p=0.001, n=54	Figure S1A (upper panel), Figure 4E-F, left panels and wings)

Table S2. V1 and V4 MUA oscillation statistics with intact V1. Related to Figure 1.

Area	Theta power increase for Kanizsa condition (mean ± SEM)	Theta power increase for control condition (mean ± SEM)	Number of channels with significant theta increase to visual stimulation ($p < 0.05$, Wilcoxon signed rank test)	Statistics (illusion> control, Wilcoxon paired signed rank test)	Gamma Power increase for Kanizsa condition (mean ± SEM)	Gamma Power increase for control condition (mean ± SEM)	Number of channels with significant theta increase to visual stimulation ($p < 0.05$, Wilcoxon signed rank)	Statistics (illusion> control, Wilcoxon paired signed rank test)	Related Figures
V1 (monkey K)	81.5 ± 2.89%	72.3±3.12%	61/61 (100%)	p=0.01, n=61	78.2±2.36%	72.6±2.39%	61/61 (100%)	p=0.03, n=61	Figure 1B
V4 (monkey B)	167.3±21.29%	128.7±28.39%	59/59 (100%)	p=1.1x10^{-5}, n=59	-	-	-	-	Figure 1C
V4 (monkey F)	79.4±16.45%	63.3±10.34%	31/54 (57%)	p=0.18, n=31	-	-	-	-	Figure S1A

Table S3. V1 and V4 LFP oscillation statistics with intact V1. Related to Figure 1.

Area	Number of channels with significant power increase to visual stimulation ($p < 0.05$, Wilcoxon signed rank test)	Number of channels with significant illusion-specific power increase ($p<0.05$, Wilcoxon rank sum test)	Statistics (illusion>control, Wilcoxon paired signed rank test)	Related Figures
Theta				
V1 (monkey K)	61/61 (100%)	3/61 (4.9%)	p=0.99, n=61	Figure 1D, S1B
V4 (monkey B)	60/60 (100%)	59/60 (98%)	p=8.4x10^{-12}, n=60	Figure 1E, S1C
V4 (monkey F)	50/60 (83%)	27/50 (54%)	p=5.9x10^{-10}, n=50	Figure S1D
Gamma				
V1 (monkey K)	61/61 (100%)	10/61 (16.4%)	p=0.97, n=61	Figure 1D, S1B
V4 (monkey B)	60/60 (100%)	36/60 (60%)	p=8.4x10^{-12}, n=60	Figure 1E, S1C
V4 (monkey F)	57/60 (95%)	47/57 (82%)	p=2.6x10^{-11}, n=57	Figure S1D

Table S4. PAC statistics with intact V1. Related to Figure 2.

Area	MI for Kanizsa condition (mean ± SEM)	MI for control condition (mean ± SEM)	Statistics (illusion>control, Wilcoxon paired signed rank test)	Number of channels with significant PAC (p<0.05, permutation test)	Number of significantly illusion-modulated channels (p<0.05, Wilcoxon rank sum test)	Mean theta phase of highest gamma amplitude (mean ± SEM, illusion condition, 0° being the theta peak)	Related Figures
V1 (monkey K)	0.050±0.0001	0.050±0.0002	p=0.055, n=61	61/61 (100%)	4/61 (6.5%)	151±6.7°	Figure 2B
V4 (monkey B)	0.045±0.0003	0.042±0.0002	p=7.7x10^{-9}, n=60	60/60 (100%)	13/60 (21.6%)	-37±2.2°	Figure 2C
V4 (monkey F)	0.044±0.0005	0.042±0.0003	p=2.2x10^{-5}, n=50	50/60 (83%)	7/50 (14%)	29±8.2°	Figure 2C

Table S5. Postlesion MUA and LFP oscillation statistics. Related to Figure 4.

Monkey	Statistics power (Pre>Post, Wilcoxon paired signed rank test)	Statistics postlesion (SNR>0, Wilcoxon signed rank test)	d' prelesion (mean ± SEM)	d' postlesion (mean ± SEM)	Statistics d' (Pre>Post, Wilcoxon paired signed rank test)	Statistics d' postlesion (d'>0, Wilcoxon signed rank test)	Related Figures
MUA – Theta							
Monkey B	$p=1.4\times10^{-6}$, n=59	$p=0.75$, n=59	0.37±0.03	-0.01±0.02	$p=8.5\times10^{-9}$, n=42	$p=0.79$, n=42	Figure 4E-F, right panels
Monkey F	$p=5.2\times10^{-4}$, n=31	$p=0.91$, n=31	0.27±0.02	-0.07±0.10	$p=0.01$, n=7	$p=0.89$, n=7	Figure 4E-F, right panels
LFP –Theta							
Monkey B	$p=8.3\times10^{-12}$, n=60	$p=0.46$, n=60	0.53±0.02	0.03±0.01	$p=1.2\times10^{-11,}$ n=59	$p=0.28$, n=59	Figure 4G-H, left panels
Monkey F	$p=4.4\times10^{-10}$, n=50	$p=0.99$, n=50	0.37±0.01	-0.14±0.03	$p=2.9\times10^{-06}$, n=27	$p=0.99$, n=27	Figure 4G-H, left panels
LFP – Gamma							
Monkey B	$p=7.6\times10^{-6}$, n=60	$p=3.9\times10^{-11}$, n=60	0.22±0.01	0.10±0.01	$p=3.3\times10^{-7}$, n=36	$p=7.4\times10^{-7}$, n=36	Figure 4G-H, right panels
Monkey F	$p=3.8\times10^{-11}$, n=57	$p=0.001$, n=57	0.34±0.01	0.12±0.02	$p=3.2\times10^{-9}$, n=47	$p=1.9\times10^{-7}$, n=47	Figure 4G-H, right panels